Journal of Materials Chemistry

Cite this: J. Mater. Chem., 2012, 22, 4881

www.rsc.org/materials

PAPER

Preparation of antibacterial surfaces by hyperthermal hydrogen induced cross-linking of polymer thin films†

Solmaz Karamdoust,[a] Binyu Yu,[b] Colin V. Bonduelle,[a] Yu Liu,[b] Greg Davidson,[ac] Goran Stojcevic,[c] Jun Yang,[b] Woon M. Lau[adef] and Elizabeth R. Gillies*[ag]

Received 11th November 2011, Accepted 19th January 2012
DOI: 10.1039/c2jm15814k

The covalent immobilization of polymers on surfaces has the potential to impart new properties and functions to surfaces for a wide range of applications. However, most current methods for the production of these surfaces involve multiple chemical steps or do not impart a high degree of control over the chemical functionalities at the surface. Described here is the preparation of surfaces covalently functionalized with quaternized poly(2-(dimethylamino)ethyl methacrylate) (PDMAEMA), a known antibacterial polymer. PDMAEMA was coated onto octadecyltrimethoxysilane modified silicon wafers and was then cross-linked by the selective cleavage of C–H bonds using a hyperthermal hydrogen treatment. The surfaces were then quaternized with ethyl bromide. At each step the surfaces were characterized extensively using techniques including atomic force microscopy, contact angle measurements and X-ray photoelectron spectroscopy. These results demonstrated a high degree of functional group retention throughout the process. The antibacterial properties of the surfaces against Gram-positive *S. aureus* and Gram-negative *E. coli* were investigated using a "drop test" assay. Furthermore, the process was successfully applied to produce antibacterial butyl rubber surfaces, demonstrating the versatility of the method for grafting onto unfunctionalized hydrocarbon surfaces.

Introduction

The immobilization of polymers on surfaces is of interest for a wide variety of applications ranging from electronic devices to biomaterials. It is of particular interest for the development of medical devices where coatings with specific properties or functions such as protein resistance,[1] antimicrobial activity,[2] and controlled drug release[3] are often desired. The immobilization of polymers on surfaces has been achieved through various processes. For example, polymers with the appropriate chemical functionalities can be grafted onto surfaces by their reaction with complementary functionalities on the surface.[4,5] Alternatively, through the conjugation of an initiator moiety to the surface, polymers can be grown from the surface.[6–9] While these approaches lead to well-defined coatings, they typically involve multi-step covalent modifications of the surfaces in order to graft the polymers or initiators, which may be an obstacle to the scaling up of these coating processes. In addition, they require the presence of reactive functionalities on the surface. In order to address this limitation, surfaces have also been generated by simple coating or painting methodologies using water insoluble polymers.[10–13] Layer by layer assembly processes using polyelectrolytes,[14,15] as well as physisorption[16] and chemisorption[17,18] have also been investigated. However, as the polymers are not covalently immobilized using these methods there may be problems associated with delamination and their long-term stability in the presence of biological fluids should be further investigated.

It is also possible to generate functional surfaces by plasma or radiation induced grafting processes.[19–21] For example, surfaces have been functionalized with poly(ethylene oxide) (PEO)[22,23] for protein resistance or polyamines[24,25] for antimicrobial properties. While careful tuning of such processes can provide well defined chemical functionalities in some cases,[26,27] many examples result

[a]Department of Chemistry, The University of Western Ontario, 1151 Richmond Street, London, Ontario, Canada N6A 5B7
[b]Department of Mechanical & Materials Engineering, The University of Western Ontario, London, Ontario, N6A 5B7, Canada
[c]LANXESS Inc., 999 Collip Circle, UWO Research Park, London, Ontario, N6G 0J3, Canada
[d]Department of Physics and Astronomy, The University of Western Ontario, 1151 Richmond Street, London, Ontario, Canada N6A 5B7
[e]Surface Science Western, 999 Collip Circle, UWO Research Park, London, Ontario, N6G 0J3, Canada
[f]Chengdu Green Energy and Green Manufacturing Technology R&D Center, Institute of Chemical Materials, China Academy of Engineering Physics, 355, 2nd Tengfei Rd, Southwest Airport Economic Development Zone, Shuangliu, Chengdu, Sichuan Province, China 610207
[g]Department of Chemical and Biochemical Engineering, The University of Western Ontario, 1151 Richmond Street, London, Ontario, Canada N6A 5B9

† Electronic supplementary information (ESI) available: ^{1}H NMR spectrum and size exclusion chromatography trace for the PDMAEMA, AFM images, additional XPS data. See DOI: 10.1039/c2jm15814k

in considerable heterogeneity in chemical functionalities at the surface, making them non-optimal for biomedical applications.[19,21,28] A method that could combine the efficiency and simplicity of plasma methods with the well defined chemical functionalities and polymer lengths afforded by the chemical immobilization approaches would provide a significant advancement.

We have recently developed a new and special plasma-based approach to synthesize molecular layers with tailor-made functionalities using the concept of collision kinematics.[29–32] This approach involves the treatment of surfaces with H_2 projectiles having appropriately elevated kinetic energy to selectively cleave C–H bonds. The treatment, therein referred to as hyperthermal hydrogen induced cross-linking (HHIC), can thus be used to covalently graft function-specific molecules to a polymer surface. In layman's terms, HHIC can be illustrated with the hard sphere approximation. According to this approximation, the maximum energy transfer between two colliding species is determined by the two masses with the formula $4M_1M_2/(M_1 + M_2)^2$. This simple model suggests that for a projectile of H_2, in the head-on collision with H of a C–H bond, the maximum kinetic energy transfer is 89%, while if the target is C, the maximum kinetic energy transfer is 49%. By considering this, as well as known bond dissociation energies, it is possible to tune the kinetic energies of the H_2 projectiles in order to afford the selective cleavage of C–H bonds on a surface. The radicals generated from the C–H bond cleavages can then combine to effectively cross-link molecular films on the surface while preserving other chemical functionalities. As a diverse array of surfaces and function-specific molecules contain C–H bonds, the HHIC method should be widely applicable.

We have recently demonstrated the use of HHIC for the preparation of PEO coated surfaces that resist the adsorption of proteins and the growth of cells[33] and for the preparation of polymer laminates based on polypropylene, butyl rubber, and poly(vinyl acetate).[34] The preparation of antibacterial surfaces using HHIC represents an ideal application, due to the diversity of chemical functionalities present in antibacterial molecules and the requirement of well-defined surfaces for biomedical applications. The development of effective antimicrobial surfaces is of significant interest for a wide range of applications. For example, the decontamination of simple objects such as doorknobs, elevator buttons, and food packaging may prevent the spread of infections in everyday life, while the use of antimicrobial medical devices such as catheters and implants may lower the rate of hospital acquired infections. The covalent immobilization of the biocide is particularly important in these applications as physical immobilization methods may lead to a gradual leaching of the antimicrobial agent from the surface, resulting in contamination of the environment, sub-inhibitory concentrations that facilitate the development of resistance, and eventually a depleted supply of biocide on the surface.[35–37] While the various grafting techniques have been used to attach antibacterial poly(quaternary ammonium) compounds to surfaces including glass,[6,8,38–40] metal,[7,41,42] silicon,[5,40] and paper,[6] these approaches are still limited by the challenges described above, and no ideal method has been developed.[2]

Thus, we describe here the use of HHIC to prepare cross-linked thin films of quaternized poly(2-(dimethylamino)ethyl methacrylate) (PDMAEMA), a known antibacterial polymer[5,6,40,43] on both a model alkane modified silicon surface as well as on butyl rubber, a common high performance elastomer. The films were extensively characterized at each step using atomic force microscopy (AFM), X-ray photoelectron spectroscopy (XPS), and contact angle measurements. The results demonstrate the effectiveness of the HHIC method in covalently immobilizing the polymer, while retaining its chemical functionality. The films are demonstrated to exhibit antimicrobial activity against both Gram-negative and Gram-positive bacteria.

Results and discussion

Preparation and characterization of functionalized silicon wafers

The steps required for the preparation of antibacterial surfaces by the HHIC process are outlined in Fig. 1. Briefly, the PDMAEMA was first spin coated onto the surface, and then was cross-linked by HHIC. The surface was washed extensively to remove any non-immobilized polymer, and then the cross-linked overlayer was quaternized by reaction with an alkyl halide. In addition to its simplicity, an advantage of this approach is that the polymer can be prepared and characterized in solution prior to its grafting onto the surface. PDMAEMA was synthesized using a previously reported method,[44] resulting in a polymer with a number average molecular weight (M_n) of 14100 g mol^{-1} and a polydispersity index (PDI) of 1.46 as determined by size exclusion chromatography in *N*,*N*-dimethylformamide (DMF) with calibration relative to polystyrene standards. The molecular weight based on end group analysis by ^{1}H NMR spectroscopy was approximately 12000 g mol^{-1}.

A silicon wafer modified with octadecyltrimethoxysilane (ODTS) was selected as a model surface for the initial series of experiments. This surface is atomically flat, thus facilitating the characterization of the polymer films by techniques such as AFM. The ODTS provides C–H bonds for the covalent cross-linking of the polymers to the surface by HHIC. In addition, it converts the highly hydrophilic silicon wafer to a hydrophobic surface, which is a better model of the hydrophobic polymer surfaces that are targeted for functionalization with antibacterial polymers. These surfaces were prepared by first cleaning the silicon wafers with a Piranha solution, then reacting them with ODTS in toluene in the presence of catalytic octylamine. The

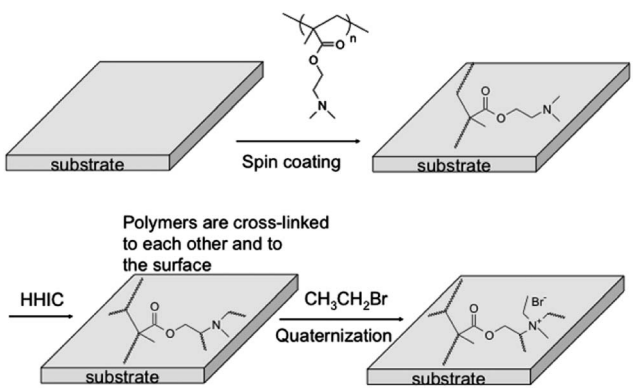

Fig. 1 Steps involved in the preparation of antibacterial surfaces using the HHIC approach.

resulting surfaces had a contact angle of (84 ± 5)° in comparison with (15 ± 3)° for the cleaned silicon surface (Table 1). In addition, as shown in Table 2, there was a significant decrease in the silicon content and an increase in the carbon content of the surface as measured by XPS.

Solutions of PDMAEMA at concentrations of 1 or 5 mg mL^{-1} in dichloromethane were then spin coated onto the modified silicon wafers. In early studies it was found that using concentrations of 1 mg mL^{-1} resulted in incomplete surface coverage. Therefore, all subsequent studies were carried out at 5 mg mL^{-1}. Following spin coating, uniform films of polymer with thicknesses from 15–25 nm were obtained, as measured by AFM (ESI†). These thicknesses are in the range appropriate for the estimated depth limit of HHIC.[29–31] The contact angle for this surface could not be determined as the non-cross-linked polymer was soluble in water. However, as shown in Table 2, XPS data revealed the presence of the PDMAEMA on the surface by the disappearance of the peak corresponding to silicon and corresponding increases in the carbon, oxygen, and nitrogen peaks from the PDMAEMA. In addition, high resolution XPS data for the C 1s region were very close to the values expected based on the chemical structure of PDMAEMA (Table 3, Fig. 2).[45,46]

The PDMAEMA coated surfaces were then cross-linked by HHIC. Treatment times of 30 and 180 s were selected in order to investigate the effect of treatment time on the structure of the PDMAEMA. In addition, while the actual degree of cross-linking cannot be quantified, it was expected that it should increase with increasing treatment times, thus resulting in polymer films with decreased chain mobility. The effect of this decrease in chain mobility on the antibacterial properties was of interest.

Following HHIC, no changes in the polymer film were observed by AFM for either the 30 or 180 s treatment time (ESI†). The contact angles of the films were measured to be (58 ± 2)° and (64 ± 5)° for the samples treated for 30 s and 180 s respectively, consistent with the previously reported contact angles of PDMAEMA functionalized surfaces.[5] XPS survey scans did not reveal any significant changes in the elemental composition of either the 30 s or 180 s samples relative to the nontreated samples. In addition, analysis of the high resolution C1s spectra (Table 3, Fig. 2) revealed that the chemical functionalities of the PDMAEMA were not significantly modified by the HHIC process.[45,46] The cross-linked films could be washed by immersion and sonication in CH_2Cl_2/NEt_3 (95/5) and the films remained intact as supported by AFM images, contact angle measurements (Table 1) and XPS (Tables 2 and 3). In contrast, when an uncross-linked film was washed under the same conditions, the AFM image showed complete removal of the material from the surface (ESI†) and the contact angle measurements and XPS results resembled those of the ODTS coated surface. Overall, these results indicate that the HHIC process was effective in covalently linking the film to the surface while retaining its chemical functionalities.

The final step for generation of the proposed antibacterial surfaces was to quaternize the tertiary amines in the PDMAEMA. This was accomplished by immersion of the surfaces in a solution of ethyl bromide in acetonitrile. Following this treatment, the contact angles dropped to (9 ± 6)° and (11 ± 4)° for the 30 s and 180 s samples respectively. These results were consistent with the expected increases in wettabilities of the surfaces due to the introduction of charged amine groups. The most notable changes in the XPS results were observed in the high resolution N 1s spectra. While only 10–20% of the N 1s peak corresponded to N^+ on the unquaternized surfaces, likely due to some degree of amine protonation, this increased to 80% following quaternization and washing (Fig. 2). The fact that a peak corresponding to unquaternized nitrogen was observed for both the 30 s and 180 s samples indicates that the reaction between the amine and ethyl bromide did not reach 100% completion. This can likely be attributed to the inaccessibility of

Table 2 XPS survey scans of surfaces

	% Composition				
	C	O	N	Si	Other
Clean silicon wafer	10	33	—	57	—
ODTS/silicon wafer	64	17	—	20	—
PDMAEMA/ODTS/silicon wafer	79	13	8	—	—
HHIC treated PDMAEMA/ODTS/silicon wafer (30 s)	79	15	6	—	
HHIC treated PDMAEMA/ODTS/silicon wafer (180 s)	78	15	7	—	
HHIC treated PDMAEMA/ODTS/silicon wafer (30 s) – washed	83	12	5	—	—
HHIC treated PDMAEMA/ODTS/silicon wafer (180 s) – washed	78	16	6	—	—
PDMAEMA/ODTS/silicon wafer – washed	62	15	1	22	—
Quaternized PDMAEMA/ODTS/silicon wafer (30 s)	78	15	5	—	2 (Br)
Quaternized PDMAEMA/ODTS/silicon wafer (180 s)	83	11	4	—	2 (Br)

Table 1 Water contact angle data for surfaces (a minimum of 5 measurements were performed on each surface)

Sample	Water Contact Angle (static)
Clean silicon wafer	(15 ± 3)°
ODTS/silicon wafer	(84 ± 5)°
PDMAEMA/ODTS/silicon wafer	Not determined (H_2O soluble)
HHIC treated PDMAEMA/ODTS/silicon wafer (30 s)	(58 ± 2)°
HHIC treated PDMAEMA/ODTS/silicon wafer (180 s)	(64 ± 5)°
HHIC treated PDMAEMA/ODTS/silicon wafer – washed (30 s)	(57 ± 4)°
HHIC treated PDMAEMA/ODTS/silicon wafer – washed (180 s)	(62 ± 4)°
PDMAEMA/ODTS/silicon wafer –washed	(85 ± 5)°
Quaternized PDMAEMA/ODTS/silicon wafer (30 s)	(9 ± 6)°
Quaternized PDMAEMA/ODTS/silicon wafer (180 s)	(11 ± 4)°

Table 3 High resolution XPS data

	% Composition of the C 1s peak			
	C–C	C–N	C–O	C=O
ODTS/silicon wafer	97	—	3	—
PDMAEMA theoretical	37.5	37.5	12.5	12.5
PDMAEMA/ODTS/silicon wafer	38	38	13	11
HHIC treated PDMAEMA/ODTS/silicon wafer (30 s)	38	37	14	11
HHIC treated PDMAEMA/ODTS/silicon wafer (30 s) – washed	39	39	11	11
HHIC treated PDMAEMA/ODTS/silicon wafer (180 s)	38	36	15	11
HHIC treated PDMAEMA/ODTS/silicon wafer (180 s) – washed	40	40	11	9
PDMAEMA/ODTS/silicon wafer – washed	99	—	1	—
	% Composition of the N 1s peak			
	C–N		C–N^+	
HHIC treated PDMAEMA/ODTS/silicon wafer (30 s) – washed	79		21	
HHIC treated PDMAEMA/ODTS/silicon wafer (180 s) – washed	90		10	
Quaternized PDMAEMA/ODTS/silicon wafer (30 s)	20		80	
Quaternized PDMAEMA/ODTS/silicon wafer (180 s)	21		79	

some amines within the polymer film following the cross-linking. Nevertheless, it would be expected that the amines at the surface of the film would be most readily quaternized in each case and these would also be most important for the antibacterial activity. To further evaluate the surface charge, the concentration of accessible quaternary ammonium groups on the surface was also quantified by a colorimetric method based on fluorescein complexation.[40] Assuming a 1 : 1 electrostatic binding between fluorescein and surface quaternary ammoniums, the surface charge density can be calculated. Using this assay, it was determined that there were 4.4×10^{15} charges/cm^2 on the surface. As this assay was performed in aqueous solution, the possible contribution of unquaternized but protonated primary amines to this value cannot be excluded but based on XPS analyses this should not contribute more than about 20% of this value. In comparison with the values obtained in previous studies, this should be sufficient for antimicrobial activity.[40]

Evaluation of the antibacterial properties of coated silicon wafers

With quaternized cross-linked films in hand, the next step was to evaluate their antibacterial properties. This was accomplished using the antibacterial "drop test" method.[47,48] Both Gram-positive *S. aureus* and Gram-negative *E. coli* were tested

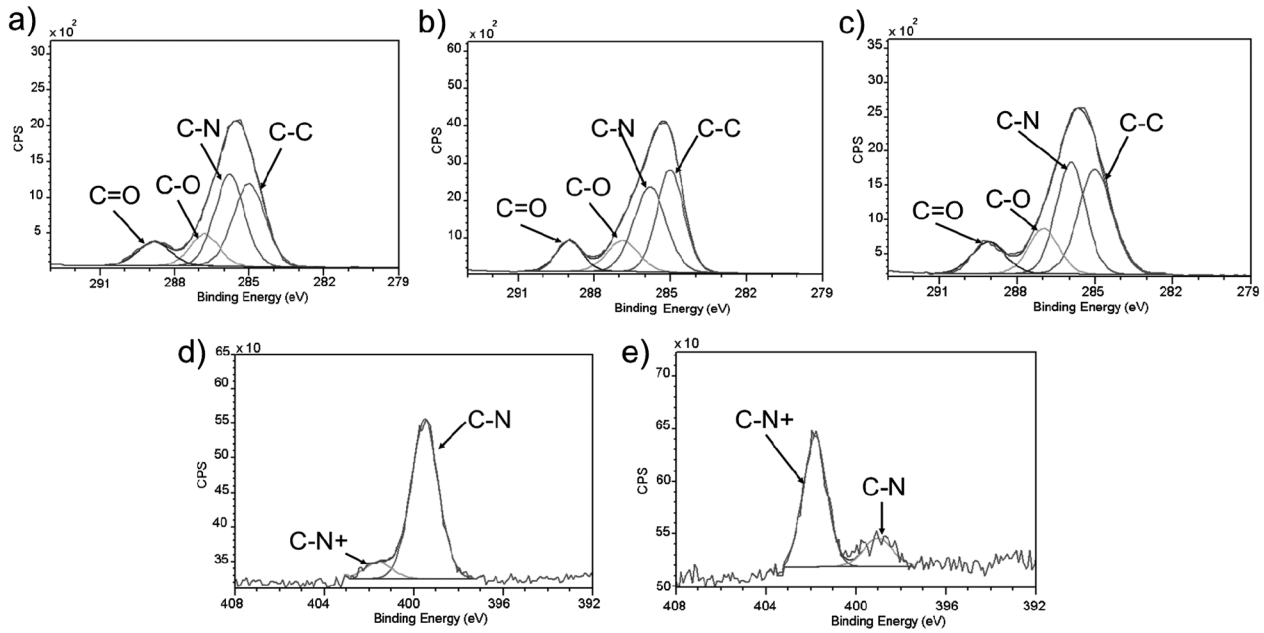

Fig. 2 High resolution XPS spectra of the C 1s region of a) PDMAEMA/ODTS/silicon wafer; b) HHIC treated PDMAEMA/ODTS/silicon wafer (30 s); c) HHIC treated PDMAEMA/ODTS/silicon wafer (180 s); and the N 1s region of d) HHIC treated PDMAEMA/ODTS/silicon wafer (180 s) e) quaternized PDMAEMA/ODTS/silicon wafer (180 s).

and the cationic surfaces were compared to clean silicon wafer controls. As shown in Table 4, the clean silicon wafer appeared based on this assay to kill or inactivate 59% of *S. aureus* and 9% of *E. coli*. The result for *S. aureus* was initially surprising but can be explained by an artifact of the assay involving the adhesion and growth of live bacteria on the surface as will be described in further detail below. The quaternized surface that was treated with HHIC for 30 s killed or inactivated 99% of *S. aureus* and 90% of *E. coli*. Increasing the cross-linking time to 180 s did not significantly change the antibacterial activities for either strain of bacteria ($p > 0.05$). Therefore, making the reasonable assumption that a greater number of cross-links are present on the surface that was treated with HHIC for 180 s, these results indicate that the expected corresponding decrease in chain mobility does not adversely affect the antibacterial activity. This is in agreement with the results of Ye *et al.* on polymer coatings prepared by vapour cross-linking.[49] In addition, it is consistent with the results of Russell and coworkers, who have found that for quaternized PDMAEMA-coated surfaces, the primary determinant in the antibacterial efficacy is the density of positive charges on the surface rather than polymer length or other properties.[5,40,43]

The activities of the surfaces towards the Gram-positive *S. aureus* relative to Gram-negative *E. coli* were not significantly ($p > 0.05$) different in the case of 180 s of HHIC treatment but the activity towards *S. aureus* was significantly ($p < 0.001$) greater for the sample treated for only 30 s. Greater activity towards *S. aureus* in comparison to *E. coli* has also been observed for other films comprising cross-linked quaternary ammonium salts[50] and thus may be related either to the particular susceptibility of the *E. coli* strain or to the mechanism of action of these surfaces in relation with the different membrane structures of Gram-positive and Gram-negative bacteria. Different mechanisms of action have been proposed for cationic surfaces including the mobilization of structurally important metal cations in the membrane,[5,38] as well as the adhesion of cationic surfaces with the anionic phospholipids resulting in disruption of the bacterial cell membrane.[51,52] The mechanism may depend on the particular surface and class of bacteria under investigation.

In order to investigate whether the apparent antibacterial activities of surfaces could be attributed to the adhesion and growth of bacteria on the surfaces, a LIVE/DEAD® BacLight Bacterial viability kit was used to visualize and differentiate between live and dead bacteria on the surface. In this assay, live bacteria appear green due to the uptake of the dye SYTO 9, which permeates all bacterial membranes, while dead bacteria appear red due to the uptake of propidium iodide which permeates only damaged bacterial membranes and dominates over the fluorescence of SYTO 9. After incubation of a clean silicon wafer with *S. aureus*, followed by rinsing of the surfaces, many live bacteria and only a very small number of dead bacteria were observed (Fig. 3). These living bacteria would be counted as killed or inactivated bacteria in the antimicrobial drop test assay as they would not be recovered from the surface for subsequent colony growth and counting. In contrast, essentially no bacteria were detected on the quaternized PDMAEMA-coated surfaces, thus confirming the true antibacterial activity.

Application to polymer surfaces

Having demonstrated that the HHIC method is an effective means of immobilizing antibacterial polymers on surfaces while retaining their activities, it was of interest to apply the method to a polymer surface. Cured butyl rubber was selected as the polymer surface for several reasons. First, commercial butyl rubber consists almost entirely of unactivated C–C and C–H bonds, making it very challenging or impossible to functionalize the surface by traditional chemical means. In contrast, the C–H

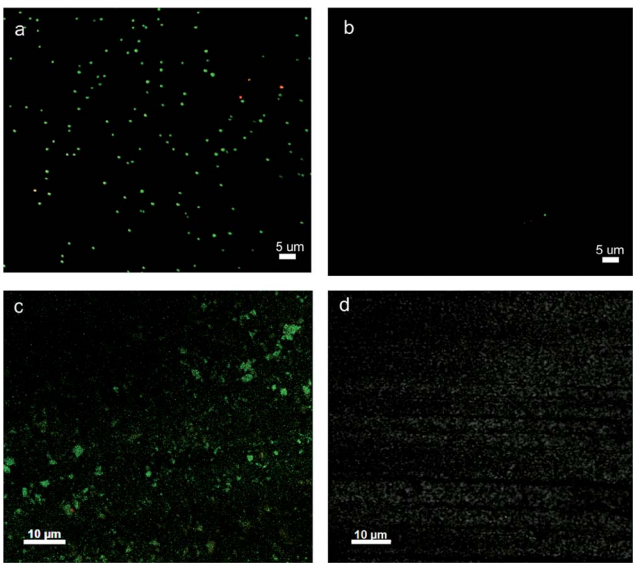

Fig. 3 LIVE/DEAD® analysis following incubation of surfaces with *S. aureus*. Live bacteria appear green in this assay, while dead bacteria appear red. a) A clean silicon wafer with many live bacteria bound; b) quaternized PDMAEMA-coated silicon surface with essentially no bound bacteria; c) cleaned butyl rubber with many live bacteria; d) quaternized PDMAEMA-coated butyl rubber with no bound bacteria detected. Note that the resolution of the butyl rubber images appears lower due to the inherent non-uniformity of the surface.

Table 4 Antibacterial activities of quaternized PDMAEMA/ODTS/silicon wafer

	% Bacteria Killed/Inactivated	
Surface	*S. aureus* (Gram-positive)	*E. coli* (Gram-negative)
Clean silicon wafer	59 ± 1	9 ± 0.1
Quaternized HHIC treated PDMAEMA/ODTS/silicon wafer (30 s)	99 ± 0.1	90 ± 1
Quaternized HHIC treated PDMAEMA/ODTS/silicon wafer (180 s)	98 ± 2	94 ± 3

bonds make it an ideal substrate for HHIC. Furthermore, butyl has recently been of interest for biomedical applications. For example, copolymers of isobutylene and styrene have been used as coatings for vascular stents, and its use in breast implants has also been proposed due to its bioinertness and high impermeability.[53–55] In order to expand the applications of butyl rubber in medical devices it may be useful to impart antibacterial properties to its surface.

Following the protocol described above for the ODTS modified silicon wafers, PDMAEMA was spin coated onto a cured sheet of butyl rubber at a concentration of 5 mg mL^{-1}. Although the low Young's modulus and non-uniformity of the surface at the nanoscale made the measurement of film thickness by AFM impossible, the C=O stretch of the carbonyl group in PDMAEMA was readily detected on the surface using attenuated total reflectance infrared spectroscopy (ATR-IR) as shown in Fig. 4. This film was cross-linked by HHIC for 30 s. Due to the non-uniformity of the surface, in order to ensure complete surface coverage, this spin coating and cross-linking procedure was performed twice. Following cross-linking, the same carbonyl peak was observed by ATR-IR and the contact angle was measured to be (63 ± 6)° in comparison with (82 ± 2)° for the initial cleaned butyl surface. This contact angle is the same as that measured for cross-linked PDMAEMA on the silicon wafer described above. Neither the ATR-IR spectrum nor the contact angle changed following washing of the cross-linked film by immersion and sonication in CH_2Cl_2/NEt_3 (95/5), indicating that the PDMAEMA was effectively immobilized. The cross-linked film was quaternized under the same conditions described above for the silicon wafers. Although no visible changes were expected or detected in the ATR-IR spectrum, a reduction in contact angle to (12 ± 6)° was measured, consistent with the presence of quaternary amines on the surface. The concentration of quaternary ammonium groups on the surface was also quantified by the fluorescein assay described above, providing a value of 5.2×10^{15} charges/cm^2 on these surfaces, similar to the value of 4.4×10^{15} charges/cm^2 obtained on the quaternized silicon wafers.

The antibacterial activities of the quaternized surfaces were measured using the same drop-test assay described above (Table 5). Butyl rubber itself was found to exhibit moderate antimicrobial activity against both *S. aureus* and *E. coli*. However, a LIVE/DEAD® BacLight Bacterial assay (Fig. 3c) revealed that this apparent activity may be due to the presence of live bacteria that adhered to the surface, as was observed for the silicon wafers. Some antibacterial activity may also be attributed to the leaching of rubber additives such as zinc oxide during the assay.[56] Upon functionalization of the surface with quaternized PDMAEMA, 93% of Gram-positive bacteria and greater than 99% of Gram-negative bacteria were killed or inactivated. No bacteria were detected on the surface using the LIVE/DEAD® assay (Fig. 3d). The results for *S. aureus* and *E. coli* are significantly ($p < 0.0001$) different, though it is not obvious why these surfaces were capable of killing or inactivating *E. coli* more effectively than the *S. aureus* while the capabilities of the coated silicon wafers were the opposite. Perhaps this points to the complexity and multiple mechanisms involved in the action of these surfaces. Nevertheless, the activities of the surfaces against Gram-negative bacteria are noteworthy and provide further evidence of the effectiveness of HHIC as a means of preparing antibacterial surfaces, even from polymer surfaces lacking reactive groups for functionalization.

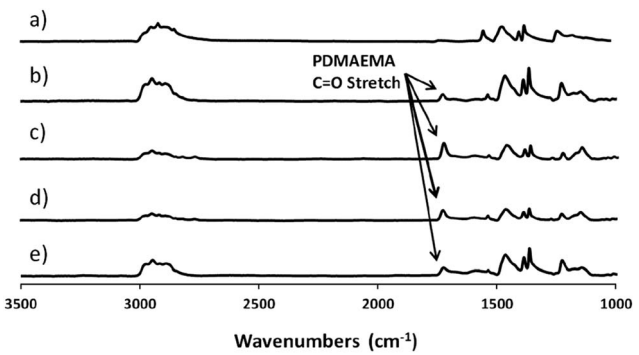

Fig. 4 ATR-IR spectra of a) butyl surface; b) PDMAEMA/butyl; c) HHIC treated PDMAEMA/butyl; d) HHIC treated PDMAEMA/butyl washed; e) quaternized HHIC treated PDMAEMA/butyl.

Conclusions

The use of HHIC as a means of cross-linking antibacterial polymers to surfaces was investigated. It was found that HHIC could be applied to ODTS modified silicon wafers coated with PDMAEMA without significant destruction of the surface or the chemical functionalities of the polymer, as evidenced by AFM, XPS, and contact angle measurements. The PDMAEMA could subsequently be quaternized to provide surfaces with high antibacterial activities against both Gram-positive *S. aureus* and Gram-negative *E. coli*. To demonstrate the full utility of the technique, HHIC was applied for the preparation of antibacterial butyl rubber surfaces. The successful application to butyl rubber, which is both nonfunctional and hydrophobic indicates that this process is likely to be very versatile and useful for the functionalization of a wide range of polymer surfaces with functional materials.

Experimental

General methods and materials

PDMAEMA was prepared as previously reported.[44] Size exclusion chromatography (SEC) was carried out in DMF with 0.1 M LiBr and 1% (v/v) NEt_3 at 85 °C using a Waters 2695 separations module equipped with a 2414 differential refractometer and two PLgel 5 μm mixed-D (300 mm × 7.5 mm) columns from Polymer Laboratories. The calibration was performed using polystyrene standards with molecular weights ranging from 580 to 170800 g mol^{-1}. All other chemicals were purchased from commercial suppliers and used as received. Silicon wafers were purchased from Solar Wafer. The grade of hydrogen gas was 99.99%. Cured butyl rubber sheets were provided by LANXESS Inc. They were cut into 1 cm × 1 cm pieces then immersed in each of ethanol, deionized water, and dichloromethane for 2 h. They were then sonicated in a 1 : 1 mixture of deionized water:ethanol for 30 min. After that they were rinsed with 1 : 1 water:ethanol, acetone, spun dry, and then left under vacuum at 40 °C overnight.

Table 5 Antibacterial activities of quaternized PDMAEMA/butyl

Surface	% Bacteria Killed/Inactivated	
	S. aureus (Gram-positive)	*E. coli* (Gram-negative)
Butyl rubber	49 ± 4	46 ± 12
Quaternized HHIC treated PDMAEMA/butyl	93 ± 0.1	>99

Modification of silicon wafers with ODTS

Silicon wafers were cut into small pieces (approximately 1.5 cm × 1.5 cm), then immersed in a 1 : 2 mixture of H_2SO_4:H_2O_2 (volume:volume) (Piranha solution; attention – strong acid, strong oxidizer!) to clean organic residues off the surface. This was followed by a thorough rinse in water and then ethanol. The wafers were then spun dry by air. A solution of toluene (25 mL), octylamine (1 drop) and octadecyltrimethoxysilane (0.5 mL) was prepared. The dried surfaces were immersed in this solution for 12 h. Finally the surfaces were washed with water and then ethanol and spun dry.

Spin coating

A 5 mg mL^{-1} solution of PDMAEMA in dichloromethane was prepared and was filtered through a 0.2 μm filter. It was then added dropwise onto the surface until it was completely covered with the solution. The surface was then spun at 4000 rpm for 15 s.

Hyperthermal hydrogen induced cross-linking (HHIC)[32]

The surfaces were treated with hyperthermal hydrogen for 30 s or 180 s. For the butyl rubber surfaces, the spin coating and cross-linking steps were carried out twice. The conditions were: (a) the hydrogen plasma was maintained with 200W of microwave energy, and 87.5 mT in magnetic field for increasing the plasma density; (b) protons were extracted by a grid electrode at −96V, into the draft tube of 50 cm at 0.80 mTorr of gaseous hydrogen; and (c) ions and electrons were screened in front of the specimen with a pair of grid-electrodes biased to +60 V and −40 V. Under this set of conditions, a high flux of hyperthermal neutral hydrogen projectiles, with appropriate kinetic energy to break C–H bonds but not other bonds undesirably, was delivered to the specimen surface. The surfaces were washed by immersion in a solution of CH_2Cl_2/NEt_3 95/5 (v/v) overnight and then in an ultrasonic bath (Fisher Scientific Ultrasonicator, model FS20H) for 30 min. Finally they were rinsed with acetone, and then ethanol, and then spun dry.

Quaternization of the PDMAEMA surfaces

The cross-linked PDMAEMA surface was placed in acetonitrile (1 mL). Excess bromoethane (0.3 mL) was added and the surfaces were agitated at a rate of 20 rpm using a GyroTwister (Labnet International Inc.) overnight at room temperature. The surfaces were then rinsed well with acetonitrile, acetone, spun dry, and then left under vacuum at 40 °C overnight.

Surface analyses

The surface topography and PDMAEMA coverage on the modified silicon wafers were analysed by AFM using a Dimension V equipped with a Nanoscope V controller from Veeco Inc. In order to determine the film thickness, a small scratch was made on the PDMAEMA down to the Si surface. AFM measurements were carried out in tapping mode using a silicon nitride cantilever tip having radius of curvature of 10 nm and a spring constant of 40 N m^{-1} under ambient conditions. XPS analyses were carried out using a Kratos Axis Ultra spectrometer using a monochromatic Al Kα source (15 mA, 14 kV) with charge neutralization. Sample data was collected at a take-off angle of 30°. CasaXPS version 2.3.14 was used for the analysis of all the XPS spectra. All spectra were referenced to the aliphatic C–H bond of 285 eV and fitting was accomplished using a Gaussian and Lorentzian ratio of 40. The binding energies at 286.9, 285.9, 286.1, 289.0 eV are attributed respectively to C–O, C–N, C–N^+, and O=C–O species of PDMAEMA.[57] Peak FWHW was constrained to fall within 0.9–1.4. All other components were allowed to freely refine. The static water contact angle of the surfaces was measured using a NRL Contact-Angle Goniometer Model 100.00. A minimum of 5 measurements were taken for each surface. Fourier transform infrared (FTIR) spectra were obtained on a Bruker IR ScopII with a micro-attenuated total reflectance (micro-ATR) attachment equipped with a germanium crystal. Areas of 80–100 μm in diameter and a depth of 1–2 μm were analyzed.

Evaluation of antibacterial properties

The antibacterial activities of the quaternized surfaces against Gram-positive bacteria *Staphylococcus aureus* (*S. aureus* ATCC3307) and Gram-negative bacteria *Escherichia coli* (*E. coli* ATCC 29425) were studied using the antibacterial drop-test.[47,48] *E. coli* or *S. aureus*, precultured in 15 mL of nutrient broth (Difco™ BD) at 37 °C for 24 h, were washed by centrifuging at 4000 rpm for 10 min. After removing the supernatant, the cells were washed with phosphate buffered saline (PBS) twice and re-suspended and diluted to approximately 3 × 10^5 colony forming units (CFU)/mL in PBS solution. The samples were placed in sterilized glass Petri dishes and sterilized by heating at 100 °C for 30 min. 100 μL of PBS solution with bacteria was added dropwise onto the surface of each sample and completely covered the sample surface. The Petri dishes were sealed and placed in an incubator at 37 °C with the humidity 46%. After 3 h, the bacteria were washed from the surface of the sample by using 10 mL PBS in the sterilized Petri dish. From this solution, 100 μL was spread onto solid plate count agar (Difco™ BD). After incubation for 24 h at 37 °C, the number of surviving bacterial colonies on the

Petri dishes were counted. The results after multiplication with the dilution factor were expressed as CFU per mL. The above experiments were carried out in triplicate for each sample. The percentage of killed/inactivated bacteria was calculated as [(CFU of initial bacterial suspension − CFUs following surface contact)/CFU of initial bacterial suspension] × 100. Results represent mean ± SD of triplicates from three separate experiments. Statistical analyses were performed using the software Prism. When comparing two data sets, unpaired, two-tailed T tests were used. When the data involved greater than two data sets an ANOVA test followed by Tukey's test was used.

LIVE/DEAD® assay

100 μL of *S. aureus* bacterial suspension (approximately 2×10^6 CFU/mL) was added drop-wise onto either a clean silicon wafer, quaternized PDMAEMA-coated silicon wafer, clean butyl rubber, or quaternized PDMAEMA-coated butyl rubber. After 3 h of incubation (at 37 °C with the humidity 46%), the surfaces were rinsed with 10 mL of PBS and 10 mL deionized water. The adherent bacteria on the surfaces were immediately stained using the LIVE/DEAD® BacLight™ Bacterial Viability Kit (Invitrogen, USA). The two BacLight stains, SYTO 9 and propidium iodide were dissolved in 0.5 mL filter-sterilized deionized water then 5 μL of each dye was diluted in 100 mL of filter-sterilized deionized water. A total of 200 μL (100 μL + 100 μL) of the dye suspension were mixed together and pipetted onto the prepared surfaces then incubated in the dark at room temperature for 15 min. Finally, the surfaces were rinsed with filter-sterilized deionized water and the fluorescence was imaged using an LSM 510 multichannel point scanning confocal microscope (Laser 488 nm for the SYTO 9 with a pass filter of 505–530 nm and a laser at 543 nm for the propidium iodide with a pass filter of 615 nm, magnification 63×). All the images were obtained and refined with the ZEN software.

Determination of surface accessible quaternary amine groups

The surface density of quaternary ammonium groups on the quaternized PDMAEMA-coated rubber surface was measured by UV-vis spectroscopy, as previously described.[40] Briefly, the surface (1×1 cm^2) was dipped in 10 mL of a 1 wt% solution of fluorescein (sodium salt) in distilled water for 10 min. The surfaces were then rinsed extensively with distilled water, placed in 3 mL of a 0.1 wt% solution of cetyltrimethylammonium chloride in distilled water, and shaken for 20 min at 300 rpm to desorb the dye. The absorbance of the resulting aqueous solution was measured at 501 nm after adding 10% v/v of 100 mM phosphate buffer (pH 8.0). The concentration of the fluorescein was calculated using an extinction coefficient of 77 mM^{-1} cm^{-1}. The conversion of the dye concentration to surface charge density was determined assuming that one surface quaternary ammonium group complexes with one dye molecule.

Acknowledgements

We thank the Natural Sciences and Engineering Research Council of Canada, and the Ontario Centers of Excellence for funding. We thank LANXESS for funding and for providing butyl rubber substrates. Mary Jane Walzak, Mark Beisinger, and Patrick Crewdson are thanked for assistance in the analysis of the XPS data.

References

1 S. Krishnan, C. J. Weinman and C. K. Ober, *J. Mater. Chem.*, 2008, **18**, 3405–3413.
2 L. Ferreira and A. Zumbuchl, *J. Mater. Chem.*, 2009, **19**, 7796–7806.
3 T. Parker, D. Vipul and R. Falotico, *Curr. Pharm. Des.*, 2010, **16**, 3978–3988.
4 S. Jo and K. Park, *Biomaterials*, 2000, **21**, 605–616.
5 J. Huang, R. R. Koepsel, H. Murata, W. Wu, S. B. Lee, T. Kowalewski, A. J. Russell and K. Matyjaszewski, *Langmuir*, 2008, **24**, 6785–6795.
6 S. B. Lee, R. R. Koepsel, S. W. Morley, K. Matyjaszewski, Y. Sun and A. J. Russell, *Biomacromolecules*, 2004, **5**, 877–882.
7 S. J. Yuan, F. J. Xu, S. O. Pehkonen, Y. P. Ting, K. G. Neoh and E. T. Kang, *Biotechnol. Bioeng.*, 2009, **103**, 268–281.
8 J. C. Tiller, C.-J. Liao, K. Lewis and A. M. Klibanov, *Proc. Natl. Acad. Sci. U. S. A.*, 2001, **98**, 5981–5985.
9 S. Edmondson, V. L. Osborne and W. T. S. Huck, *Chem. Soc. Rev.*, 2004, **33**, 14–22.
10 J. Haldar, D. An, L. Alvarez de Cienfuegos, J. Chen and A. M. Klibanov, *Proc. Natl. Acad. Sci. U. S. A.*, 2006, **103**, 17667–17671.
11 A. D. Fuchs and J. C. Tiller, *Angew. Chem., Int. Ed.*, 2006, **45**, 6759–6762.
12 S. Krishnan, R. J. Ward, A. Hexemer, K. E. Sohn, K. L. Lee, E. R. Angert, D. A. Fischer, E. J. Kramer and C. K. Ober, *Langmuir*, 2006, **22**, 11255–11266.
13 D. Park, J. Wang and A. M. Klibanov, *Biotechnol. Prog.*, 2006, **22**, 584–589.
14 J. A. Lichter, K. J. Van Vliet and M. F. Rubner, *Macromolecules*, 2009, **42**, 8573–8586.
15 S.-Y. Wong, J. S. Moskowitz, J. Veselinovic, R. A. Rosario, K. Timachova, M. R. Blaisse, R. C. Fuller, A. M. Klibanov and P. T. Hammond, *J. Am. Chem. Soc.*, 2010, **132**, 17840–17848.
16 J. H. Lee, J. Kopecek and J. D. Andrade, *J. Biomed. Mater. Res.*, 1989, **23**, 351–368.
17 L. D. Unsworth, H. Sheardown and J. L. Brash, *Biomaterials*, 2005, **26**, 5927–5933.
18 K. L. Prime and G. M. Whitesides, *J. Am. Chem. Soc.*, 1993, **115**, 10714–10721.
19 K. S. Siow, L. Britcher, S. Kumar and H. J. Griesser, *Plasma Processes Polym.*, 2006, **3**, 392–418.
20 I. P. Jain and G. Agarwal, *Surf. Sci. Rep.*, 2011, **66**, 77–172.
21 T. Desmet, R. Morent, N. De Geyter, C. Leys, E. Schacht and P. Dubruel, *Biomacromolecules*, 2009, **10**, 2351–2378.
22 M. S. Sheu, A. S. Hoffman and J. Feijen, *J. Adhes. Sci. Technol.*, 1992, **6**, 995–1009.
23 R. A. D'Sa and B. J. Meenan, *Langmuir*, 2010, **26**, 1894–1903.
24 S. Tan, G. Li, J. Shen, Y. Liu and M. Zong, *J. Appl. Polym. Sci.*, 2000, **77**, 1869–1876.
25 S. N. Jampala, M. Sarmadi, E. B. Somers, A. C. L. Wong and F. S. Denes, *Langmuir*, 2008, **24**, 8583–8591.
26 E. J. Kinmond, C. S. R., J. P. S. Badyal, B. S. A. and C. Willis, *Polymer*, 2005, **46**, 6829–6835.
27 L. J. Ward, W. C. E. Schofield, J. P. S. Badyal, A. J. Goodwin and P. J. Merlin, *Chem. Mater.*, 2003, **15**, 1466–1469.
28 B. J. Ringrose and E. Kronfli, *Eur. Polym. J.*, 2000, **36**, 591–599.
29 Z. Zheng, X. D. Xu, F. X.L., W. M. Lau and R. W. M. Kwok, *J. Am. Chem. Soc.*, 2004, **126**, 12336–12342.
30 Z. Zheng, R. W. M. Kwok and W. M. Lau, *Chem. Commun.*, 2006, 3122–3124.
31 Z. Zheng, K. W. Wong, W. C. Lau, R. W. M. Kwok and W. M. Lau, *Chem.–Eur. J.*, 2007, **13**, 3187–3192.
32 Y. Liu, D. Q. Yang, H.-Y. Nie, W. M. Lau and J. Yang, *J. Chem. Phys.*, 2011, **134**, 074704.
33 C. Bonduelle, W. M. Lau and E. Gillies, *ACS Appl. Mater. Interfaces*, 2011, **3**, 1740–1748.
34 D. B. Thompson, T. Trebicky, P. Crewdson, M. J. McEachran, G. Stojcevic, G. Arsenault, W. M. Lau and E. R Gillies, *Langmuir*, 2011, **27**, 14820–14827.
35 A. W. Smith, *Adv. Drug Delivery Rev.*, 2005, **57**, 1539–1550.

36 D. M. Drekonja, M. A. Kuskowski, T. J. Wilt and J. R. Johnson, *Expert Rev. Med. Devices*, 2008, **5**, 495–506.
37 R. O. Darouiche, M. D. Mansouri and E. M. Kojic, *Clin. Microbiol. Infect.*, 2006, **12**, 397–399.
38 R. Kugler, O. Bouloussa and F. Rondelez, *Microbiology*, 2005, **151**, 1341–1348.
39 N. M. Milovic, J. Wang, K. Lewis and A. M. Klibanov, *Biotechnol. Bioeng.*, 2005, **90**, 715–722.
40 H. Murata, R. R. Koepsel, K. Matyjaszewski and A. J. Russell, *Biomaterials*, 2007, **28**, 4870–4879.
41 S. J. Yuan, S. O. Pehkonen, Y. P. Ting, K. G. Neoh and E. T. Kang, *Langmuir*, 2010, **26**, 6728–6736.
42 M. Ignatova, S. Voccia, B. Gilbert, N. Markova, P. S. Mercuri, M. Galleni, V. Sciannamea, S. Lenoir, D. Cossement, R. Gouttebaron, R. Jerome and C. Jerome, *Langmuir*, 2004, **20**, 10718–10726.
43 J. Huang, H. Murata, R. R. Koepsel, A. J. Russell and K. Matyjaszewski, *Biomacromolecules*, 2007, **8**, 1396–1399.
44 W. Agut, D. Taton and S. Lecommandoux, *Macromolecules*, 2007, **40**, 5653–5661.
45 G. Beamson; D. Briggs. *High Resolution XPS or Organic Polymers -The Scienta ESCA300 Database*; John Wiley and Sons: London, 1992.
46 B. V. Christ. *Handbook of Monochromatic XPS Spectra - The Elements of Native Oxides*; John Wiley and Sons, 1999.
47 L. Cen, K. G. Neoh and E. T. Kang, *Langmuir*, 2003, **19**, 10295–10303.
48 J. Fu, J. Ji, W. Yuan and J. Shen, *Biomaterials*, 2005, **26**, 6684–6692.
49 Y. Ye, Q. Song and Y. Mao, *J. Mater. Chem.*, 2011, **21**, 257–262.
50 M. Saif, J. Anwar and M. A. Munawar, *Langmuir*, 2009, **25**, 377–379.
51 A. M. Bieser and J. C. Tiller, *Macromol. Biosci.*, 2011, **11**, 526–534.
52 K. Lewis and A. M. Klibanov, *Trends Biotechnol.*, 2005, **23**, 343–348.
53 J. E. Puskas and Y. Chen, *Biomacromolecules*, 2004, **5**, 1141–1154.
54 J. E. Puskas, Y. Chen, Y. Dahman and D. Padavan, *J. Polym. Sci., Part A: Polym. Chem.*, 2004, **42**, 3091–3109.
55 L. Pinchuk, G. J. Wilson, J. J. Barry, R. T. Schoephoersterd, J. M. Parele and J. P. Kennedy, *Biomaterials*, 2008, **29**, 448–460.
56 W. R. Moore and J. M. Genet, *Oral Surg., Oral Med., Oral Pathol.*, 1982, **53**, 508–517.
57 J. F. Moulder; W. F. Stickle; P. E. Sobol; K. D. Bomben. *Handbook of X-Ray Photoelectron Spectroscopy*; Perkin-Elmer Corp: Eden Prairie, MN, 1992.